Quantum tunneling time: Insights from an exactly solvable model

S. Yusofsani and M. Kolesik
College of Optical Sciences, University of Arizona, Tucson, Arizona 85721, USA

(Received 28 September 2019; revised manuscript received 4 February 2020; accepted 15 April 2020; published 27 May 2020)

Quantum particles interacting with potential barriers are ubiquitous in physics, and the question of how much time they spend inside classically forbidden regions has attracted interest for many decades. Recent developments of new experimental techniques revived the issue and ignited a debate with often contradictory results. This motivates the present study of an exactly solvable model for quantum tunneling induced by a strong field. We show that the tunneling dynamics can depart significantly from the scenario in which the barrier-traversal time is zero or very small. However, our findings do not support the idea of a well-defined tunneling time either. Our numerically exact results should help in finding a consensus about this fundamental problem.

DOI: 10.1103/PhysRevA.101.052121

I. INTRODUCTION

The tunnel effect [1–3] has captured the imagination of physicists from the early days of quantum mechanics. Perhaps because of the lack of a classical analog, one question in particular attracted a great deal of attention, namely, how long a quantum particle spends inside a potential barrier (see, e.g., [4–6]), i.e., in the spatial region that is inaccessible to it in classical physics. This problem was studied numerous times [7] in various physical contexts from the scattering on a one-dimensional potential barrier [8] to the mapping of electron trajectories in attosecond angular streaking experiments [9,10].

It is fair to say that the physics community has not yet completely agreed on the answer. On the contrary, recent development of ultraprecise techniques in strong-field physics [9,11] reignited the debate as experiments produced often contradictory results.

The literature dealing with the tunneling dynamics is extensive. To give a few representative examples, there are, very roughly speaking, three schools of thought concerning the subject. Some experiments produced evidence that the time needed to traverse a potential barrier is zero, negligible [11–14], or at least very small [15]. Others maintain that it takes a certain finite amount of time before a particle emerges from its quantum tunnel through a potential barrier [10,16–20]. Yet other authors hold the idea that characterization in terms of a sharply defined tunneling time is not suitable or useful for what is an inherently nonclassical effect [21,22].

One possible reason that this controversy is difficult to settle is that sophisticated strong-field experiments [9,11] require an interpretation model [23] to give a meaning to the measured data, e.g., one has to map the location of a detected free electron to its classical trajectory [13,14] in order to deduce the time at which the electron was released from an atom. Theoretical approaches, such as numerical solutions to the time-dependent Schrödinger equation [24,25], have their own challenges too. Subtle differences between definitions, including traversal, dwell, and reflection times [8], as well as the point of exit [14,26] and multielectron effects [27] add further dimensions to the discussion. Some of the frequently discussed approaches for the tunneling time are the Larmor time, Büttiker-Landauer time [6], Eisenbud-Wigner time [28], Pollak-Miller time [29], Wigner time [30], and Bohmian time [31,32]. While the first four of these do not have a straightforward application in the situation discussed in this work (due to differences in the physical setting and/or simplicity of our model), Wigner and Bohmian times could apply to our scenario, with the Wigner time being perhaps the most relevant.

Inspired by the ongoing debate, we present a theoretical study of a simple but exactly solvable model that allows one to accurately characterize the time-dependent wave function of a tunneling particle. Of course, simple systems have been employed in this problem before (see, e.g., [33]; also, the scenario investigated in [34] is similar in spirit to ours). Here we want to concentrate on tunneling invoked by an external field. Our approach makes it possible to study the dynamics in the regime of a nearly opaque, spatially very long barrier that is difficult to address by other methods and which greatly emphasizes the quantum nature of the effect. In particular, we are able to investigate the dynamics for very weak field strengths, where the distinction between instantaneous and delayed tunneling is clearer and where it is easier to identify the effective exit point from the quantum tunnel.

II. MODEL

The rationale for choosing the model for our investigation is the need to eliminate the uncertainties that one inevitably encounters in the numerical solution and in the interpretations of results for a more realistic system. We consider a toy model that can be solved exactly and the solution of which can be accurately evaluated numerically. Let us assume a Stark problem given by a Hamiltonian for a one-dimensional particle,

$$H = -\frac{1}{2}\frac{d^2}{dx^2} - V_0 \quad \text{for} \quad -L \leqslant x \leqslant 0,$$
$$H = -\frac{1}{2}\frac{d^2}{dx^2} - Fx \quad \text{for} \quad x > 0, \tag{1}$$

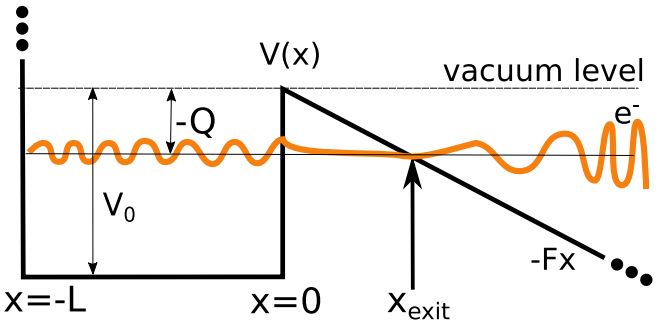

FIG. 1. Potential function for a one-dimensional model of a metal nanotip. For the initial condition given by a zero-field stationary state with energy $-|Q|$, we aim to calculate the time-dependent wave function of the tunneling particle for locations beyond the classical tunnel exit at x_{exit}.

where the field strength $F > 0$ and the depth of the potential well in the left half space is constant (with positive V_0). To select the domain of the Hamiltonian (1), we assume $\partial_x \psi(x = -L) = 0$. At $x = 0$ we require the functions belonging to the domain of the operator to be continuous, together with their first derivative.

This model is inspired by a metal nanotip exposed to a strong external field as realized in experiments by irradiation by strong optical pulses [35,36]. Here we consider a constant field strength and concentrate on timescales much shorter than the optical cycle. The potential well represents a partially filled conduction band, so the energy of $W = -V_0$ represents the bottom of the band and the states in the vicinity of the Fermi level will contribute the most to the tunneling current. While the limit $L \to \infty$ can be taken, we will evaluate our illustrations for a finite L and note that a concrete choice of its value plays no significant role in our observations.

We will examine this model also in a complementary limit representing a different physical situation. Namely, we take a small-L and large-V_0 limit such that there exists exactly one bound state with energy equal to $-1/2$. This is to mimic quantum tunneling from atoms exposed to strong fields.

The scenario we are to examine is as follows. We assume that the system is prepared in the absence of the external field, i.e., we have $F = 0$, and the initial wave function is selected as one of the bound eigenstates. We denote its energy by Q.

Then, at time $t = 0$ we suddenly switch the field on to $F > 0$ and then follow the evolution of the wave function. Any positive value of the the field strength F creates a finite but possibly broad potential barrier through which the initial state can tunnel toward $x \to \infty$. We are particularly interested in how long it takes for the particle to appear at the classical exit from the tunnel, i.e., at the location $x_{\text{exit}} = -Q/F$. More generally, it is desirable to understand the dynamics of the wave function in the classically allowed region $\psi(x > x_{\text{exit}}, t > 0)$. For example, from the application standpoint it is important to understand the emitted electron bunches, including any limits for the duration of such pulses. The situation is schematically depicted in Fig. 1.

A. Initial wave function

The initial condition is a zero-field eigenfunction corresponding to a negative energy $Q \in (-V_0, 0)$. Convenient parametrization, utilizing a real-valued wave number $k_Q = \sqrt{2(V_0 + Q)}$, can be written as

$$\psi_Q(x) = \frac{\cos(k_Q(L + x))}{\cos(k_Q L)} \quad \text{for } x < 0,$$
$$\psi_Q(x) = \exp(-\sqrt{-2Q}x) \quad \text{for } x > 0 \tag{2}$$

and the eigenvalue equation for energy Q is

$$k_Q \tan(k_Q L) = \sqrt{-2Q}. \tag{3}$$

The evolution of the system starts from such a bound state after a sudden switch of the field F from zero to a finite positive value. The instantaneous switching on of the field gives a clear meaning to the time when the evolution starts. If there were a finite ramping time of $F(t)$, it would not be clear at what exact time the tunneling process commences. Despite the fact that the tunneling probability grows exponentially with the field, the ramp inevitably introduces an uncertainty into the interpretation of $t = 0$. On the other hand, for an instantaneous turn-on of the field, the dynamics we are going to encounter is nonadiabatic, as we will appreciate shortly.

B. Spectrum and eigenfunctions in a nonzero field

Needless to say, ours is a textbook, exactly solvable system for which all Hamiltonian eigenstates can be easily obtained. For any positive F, however small, the spectrum of our system becomes continuous and it encompasses the whole real axis. The following is a suitable parametrization of the energy eigenfunctions we will utilize in what follows:

$$H\psi_W(x) = W\psi_W(x),$$
$$\psi_W(x) = \frac{\cos[k_W(L + x)]}{\cos(k_W L)} \frac{1}{N\sqrt{D^+ D^-}} \quad \text{for } x < 0,$$
$$\psi_W(x) = -\frac{i}{N}\sqrt{\frac{D^-}{D^+}}\text{Ci}^+[\alpha(x + W/F)]$$
$$+ \frac{i}{N}\sqrt{\frac{D^+}{D^-}}\text{Ci}^-[\alpha(x + W/F)] \quad \text{for } x > 0. \tag{4}$$

Here $k_W = \sqrt{2(V_0 + W)}$, $\alpha = -(2F)^{1/3}$, and $N = 2^{7/6}F^{1/6}$ is a normalization factor. The functions $\text{Ci}^{\pm}$ are linear combinations of the Airy functions

$$\text{Ci}^{\pm}(z) = \text{Bi}(z) \pm i\,\text{Ai}(z) \tag{5}$$

and are chosen as such in order to express ψ_W as a superposition of the incoming and outgoing waves. Specifically, $\text{Ci}^+[\alpha(x + W/F)]$ behaves as an outgoing wave in the region of large positive x.

Functions $D^{\pm}(W)$ are determined from the requirement of smoothness at $x = 0$. Asking for the continuity of the wave

function and of its first derivative at $x = 0$, one obtains

$$D^+(W) = \frac{\pi}{2}\left(\mathrm{Ci}^{+'}(\alpha W/F) + \frac{k_W}{\alpha}\tan(k_W L)\mathrm{Ci}^{+}(\alpha W/F)\right),$$
$$D^-(W) = \frac{\pi}{2}\left(\mathrm{Ci}^{-'}(\alpha W/F) + \frac{k_W}{\alpha}\tan(k_W L)\mathrm{Ci}^{-}(\alpha W/F)\right). \tag{6}$$

Note that the zeros of these expressions, when analytically continued to the complex plane, determine the location of the Stark resonances for the model under consideration. When $W = z$ is chosen such that $D^+(z) = 0$, the incoming part of the wave function vanishes, while the outgoing one has poles at complex-valued energies. We will utilize the outgoing resonances to construct part of the wave function of the particle as it tunnels through the potential barrier.

Note that the atom-model limit of $L \to 0$ and $V_0 \to \infty$ can be taken in the above formulas by taking

$$k_W \tan(k_W L) \to 1. \tag{7}$$

This limit introduces a contact or Dirac-delta interaction at the origin and fixes the energy of the single bound state to $-1/2$.

C. Expansion in energy eigenstates

We start with the formulation of the time-dependent solution in the standard way, using the completeness of the Hamiltonian eigenfunctions. The eigenstates $\psi_W(x)$ can be normalized to the Dirac-delta function in energy W so that we have a unity decomposition guaranteed to exist for the self-adjoint operator

$$\int \psi_W(x)\psi_W(y)dW = \delta(x-y), \tag{8}$$

which is the completeness relation that allows one to express an arbitrary initial wave function $\phi(x)$ as

$$\phi(x) = \int \delta(x-y)\phi(y)dy = \int \psi_W(x)\int \psi_W(y)\phi(y)dy\,dW, \tag{9}$$

where we use the fact that ψ_W is real. The evolution of this initial condition at later times can be described with the expansion written as

$$\psi(x,t) = \int \frac{e^{-itW}\psi_W(x)}{\sqrt{D^-(W)D^+(W)}}A(W)dW, \tag{10}$$

with the overlap integral

$$A(W) = \int \sqrt{D^-(W)D^+(W)}\psi_W(y)\phi(y)dy. \tag{11}$$

The $D^\pm$ factors are distributed in the above such that we have analytic functions when continued into the complex plane.

Interested in the tunneling part of the solution for $x > 0$, we can write the outside component as

$$\psi = \int \frac{ie^{-itW}}{N}\left[\frac{\mathrm{Ci}^-\left(\alpha x + \frac{\alpha W}{F}\right)}{D^-(W)} - \frac{\mathrm{Ci}^+\left(\alpha x + \frac{\alpha W}{F}\right)}{D^+(W)}\right]A(W)dW. \tag{12}$$

The spectral amplitude $A(W)$ can be split into $A(W) = A_{\mathrm{I}}(W) + A_{\mathrm{O}}(W)$, where the overlap integral between ψ_W and ϕ consists of the inside and outside (of the well) contributions. Specializing this for the chosen initial wave function $\psi_Q(x)$, we have an exact

$$A_{\mathrm{I}} = \frac{\sqrt{-2Q} - k_W\tan(k_W L)}{2N(Q-W)} \tag{13}$$

and

$$A_{\mathrm{O}} = -\frac{i}{N}\int_0^\infty dy\exp(-\sqrt{-2Q}y)\left\{D^-(W)\mathrm{Ci}^+\left[\alpha\left(y+\frac{W}{F}\right)\right] - D^+(W)\mathrm{Ci}^-\left[\alpha\left(y+\frac{W}{F}\right)\right]\right\}, \tag{14}$$

which must be calculated numerically.

D. Expansion in resonant states

The expansion of the time-dependent wave function in terms of energy eigenstates (12) can in principle be evaluated. Unfortunately, numerical calculation of the integral in (12) is next to impossible due to extremely fast variation of the integrand. This is a challenge especially for a very weak field F that pulls the arguments of the embedded Airy functions to infinity. The fast integrand variation is caused by poles located extremely close to the real axis. These poles correspond to the Stark resonances, which may be viewed as eigenstates of a non-Hermitian Hamiltonian which has the same differential expression as (1) but has its domain specified by the asymptotic boundary condition which requires that the functions that belong to the domain behave as outgoing waves (also known as the Siegert boundary condition).

We proceed to evaluate the formally exact expression for $\psi(x,t)$ by deforming the integration contour from that following the real axis to one for which the difficult to calculate part of the integral can be obtained from the Stark poles. We choose an integration contour $C = \{z \in \mathbb{C}; \mathrm{Im}\{z\} = -s\}$ that parallels the real axis in the lower complex half plane. Utilizing the residue theorem, the expression for the outside wave function can be written as

$$\psi(x,t) = -2\pi\sum_p e^{-itW_p}\frac{\mathrm{Ci}^+[\alpha(x+W_p/F)]}{ND^{+'}(W_p)}A(W_p) + \int_C \frac{ie^{-itz}}{N}\left[\frac{\mathrm{Ci}^-\left(\alpha x+\frac{\alpha z}{F}\right)}{D^-(z)} - \frac{\mathrm{Ci}^+\left(\alpha x+\frac{\alpha z}{F}\right)}{ND^+(z)}\right]A(z)dz. \tag{15}$$

Here the set of poles W_p that were crossed by deformation of the contour is finite and it depends on the choice of the parameter s. The discrete sum above is a resonant-state expansion and its purpose here is to replace the part of the integral that is most difficult to evaluate.

Resonant series expansions similar to the discrete part of (15) were successfully used in systems exhibiting spontaneous decay without the external field (see, e.g., [37]). The situation is somewhat different for the Stark resonant states that arise due to the homogeneous external field. We therefore think it may be illustrative to discuss the general structure of the poles that are relevant for our resonant-state series.

There are three families of poles distributed in the lower half of the complex plane (with their counterparts related to

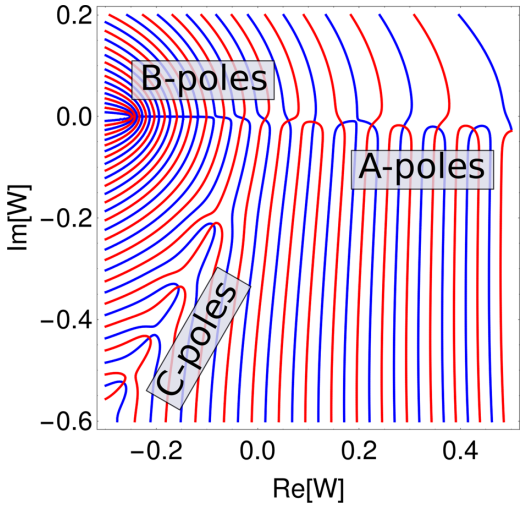

FIG. 2. Solutions to the resonant-state eigenvalue equations. The contours are zero lines for the real and imaginary parts of $D^+(W)$ and their intersections indicate the location of the resonant poles W_p. Three different families of solutions are indicated here and discussed in the text.

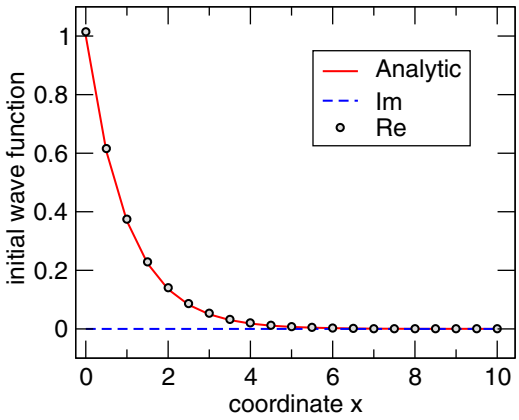

FIG. 3. Initial wave function of the particle as reproduced by the mixed representation utilizing a contour integral and a subset of outgoing resonant states (15).

the incoming resonant states existing in the upper half plane). They are illustrated in Fig. 2. The figure shows the contours defined by $\mathrm{Re}\{D^+(W)\} = 0$ in blue and $\mathrm{Im}\{D^+(W)\} = 0$ in red. Thus, the intersections of these contours mark the locations of the resonant-state poles. The first set is the B poles; they correspond to the metastable states that arise from the zero-field bound states. The imaginary parts of these complex energies are tiny and therefore invisible on the scale of this figure. The second set of poles, marked with A in the figure, corresponds to the resonant states similar to the positive-energy states at $F = 0$. There are infinitely many of these poles, located below the real axis, with the imaginary part growing for the resonances with larger real parts. The third set of poles, indicated by C in the picture, is located along the Stokes line of Airy functions. Again, there are infinitely many of them, each in the vicinity of zeros of $\mathrm{Ci}^+(\alpha z/F)$.

It should be noted that the parameters for this illustration were chosen such that only a few poles appear in each family. Specifically, this requires an extremely strong field and a small potential well that only accommodates a few bound states.

We choose our contour C to run close to the real axis, but below B poles. As C continues into the half plane $\mathrm{Re}\{z\} > 0$, it eventually crosses the line of A poles, so the resonant-state expansion part of (15) is limited to those poles that are located between the real axis and contour C. The specific choice of C is informed by the numerics involved. As the contour drops deeper into the lower plane, the influence of the B poles becomes less severe and their contribution is replaced by the resonant-state sum. However, Airy functions grow exponentially fast away from the real axis, which means that there exist huge cancellations in the numerical evaluation of various terms contributing to the contour integral. It is therefore most practical to keep C not too distant from the real axis. The results shown here were obtained with $s = 3/100$, which required about 60 poles contributing to the resonant-state series. We have performed all our calculations for several different values of s in order to verify that the results are indeed independent of the choice for the contour.

III. RESULTS

A. Tunneling from a discrete state

We start our illustrations with the atom-model case since it is much less computationally demanding. For this we take the large-V_0 plus small-L limit specified in (7) so that there remains a single bound state with an energy of $Q = -1/2$ and the wave function $\phi(x) = e^{-x}$, which serves as our initial condition.

In order to check that our expansion and numerical integration in (15) are properly normalized and can be evaluated with sufficient accuracy, we verify that for $t = 0$ we indeed recover the initial wave function. This is illustrated in Fig. 3. The imaginary part of the recovered wave function should vanish, and our calculations give values of the order of 10^{-8}. The error in the real part is on the level of a percent at the origin where it is largest.

Concentrating on the question of the tunneling time, we observe the probability density as it evolves at a fixed point of observation. If one assumes that the so-called simple-man's picture of quantum tunneling applies, then we expect that the particle appears at $x_{\mathrm{exit}} = -Q/F$ instantaneously and it has zero velocity at the exit from the tunnel. Then, subject to acceleration by the external field, it moves away and arrives at a chosen observation location x_{obs}. The expected time of arrival based on this scenario is $t_{\mathrm{eta}} = \sqrt{2(x_{\mathrm{obs}} - x_{\mathrm{exit}})/F}$.

First we evaluate the full wave function at the position $x = 25$, which corresponds to the classical exit from the tunnel for the given applied field $F = 1/50$. Figure 4 shows that the tunneling particle appears at the classical exit not instantaneously, but delayed. The real and imaginary parts of the wave function evaluated versus the observation time indicate that at earlier times the particle arrives most likely with a higher velocity than at later times. This is in line with previous works, e.g., [38], that have also shown that for a one-dimensional model the tunneling ionization produces a nonzero outgoing momentum at the tunnel exit. Clearly, the simple-man's scenario does not apply to this specific situation

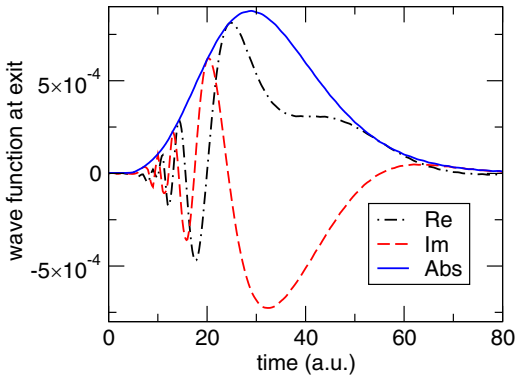

FIG. 4. Tunneling from a single bound state. The particle wave function is shown versus time at the location corresponding to the classical tunnel-exit point.

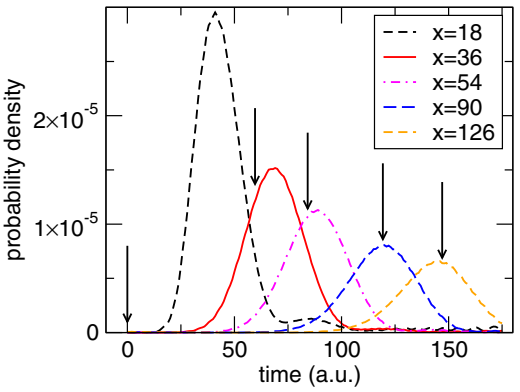

FIG. 6. Tunneling particle probability density versus time for different observation locations x. Arrows mark the expected time of arrival for a particle that obeys the simple-man's scenario.

as there is a pronounced delay and the arrival time exhibits a broad distribution.

In order to appreciate the arrival timing of the particle at different observation locations, Fig. 5 depicts the observed probability density versus time as detected at two locations. Arrows mark the expected time of arrival at the given location under the assumption that the simple man's scenario holds. When the peak of the probability density pulse is adopted as the location of the classical trajectory, it becomes evident that the particle arrives early at more distant locations, indicating that the initial velocity at the classical exit does not vanish, which is also in contrast to the simple-man's scenario.

B. Tunneling from a quasicontinuum of states

To illustrate our observations concerning the dynamics of the tunneling particle for the model of a metal nanotip, we choose $L = 100$, $V_0 = 25/68$, $Q = -0.1848\ldots$, and a very weak field $F = 1/100$. The depth of the potential well V_0 and the energy Q of the initial stationary state are motivated by metal nanotips, with Q taken roughly corresponding to the typical work function of common metals. In contrast, the above field value (in atomic units) is significantly smaller than the typical fields achieved by irradiation by femtosecond optical pulses. As alluded to in the Introduction, we concentrate on weak fields in order to make the potential barrier nearly opaque and thus amplify the potential deviations from the scenario of the instantaneous tunneling.

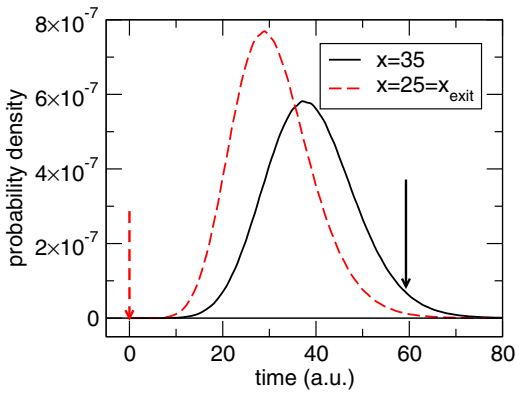

FIG. 5. Tunneling particle probability density versus time for two different observation locations x for a model with a single bound state taken as the initial wave function. The dashed line corresponds to the location at the classical tunnel exit. Arrows mark the expected time of arrival for a particle that obeys the simple-man's scenario.

The first step in numerical evaluation of the expansion in (15) is to obtain the locations of poles, or solutions to the equation $D^+(W) = 0$. This can be done by initiating the search around the energies close to the bottom of the potential well. Having found two and more poles, one can estimate the location of the next by extrapolation and subsequently find the root with working precision of up to 200 digits. The high numerical accuracy during this and subsequent calculations is a must in order to obtain converged results. Depending on the contour chosen, several tens of resonant poles W_p are needed for the chosen size of the potential well.

The next step consists in calculating the different terms that originate in the integrand of (14), in particular the wave-function overlaps $A(W_p)$ and the pole-residue values $D^{+'}(W_p)$. Obviously, high-precision arithmetic must be employed. Having found the complex resonant energies and the corresponding wave-function overlaps together with the pole residues, we can evaluate the resonant-expansion part of the wave function.

Evaluation of the contour integral is straightforward but it requires a great deal of numerical effort. We found that accurate tabulation of the integrand along the contour with very fine discretization along z helps to speed up the calculation for the wave function as a function of time.

Figure 6 shows selected results for one of our simulations. For the chosen parameters, the exit from the tunnel is at $x_{\rm exit} = 18$; the dashed black curve corresponds to this observation location. It reveals that the maximum of the probability density arrives significantly delayed with respect to $t_{\rm eta} = 0$. Obviously, in this case the tunneling time seems to be finite and in fact rather far from instantaneous.

Several other curves in Fig. 6 show similar results for the observation locations at increasing distances from the tunnel exit. The arrows in the plot indicate the expected time of arrival in each case. One can see that while the particle seems to be delayed when observed close to the tunnel exit, it arrives earlier than expected when detected far from the tunnel. In

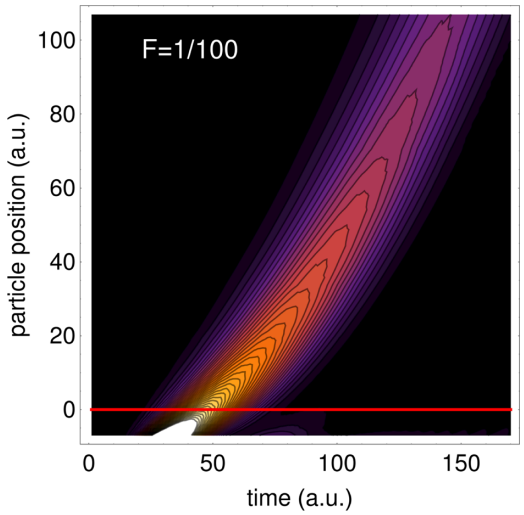

FIG. 7. Probability density for the tunneling particle versus time and observation location. The red horizontal line indicates the location of the tunnel exit for the given external field strength.

other words, it moves faster than expected; this is due to the fact that, contrary to the simple-man's model, it exhibits a nonzero velocity at the exit. One could argue that the classical exit point x_{exit} must not be taken as given by the nominal value $-Q/F$, but should be adjusted. Indeed, a classical trajectory fitted to our numerical results would indicate the effective tunnel-exit point at $x \sim 5$ and an escape velocity of 0.12 a.u.

A note concerning the interpretation of the curves shown in Fig. 6 might be in order. The figure shows that the amplitude of the pulse decreases with the distance from the origin, while the duration only increases slowly. It might therefore seem that the total probability of finding the particle inside the pulse may not be conserved. However, one has to consider the fact that the particle accelerates in the external field and the pulse in fact delivers the same accumulated probability independently of the distance. This can be verified accurately when the wave function (or, more accurately, the probability density) is integrated over space for a fixed time. In our illustration the probability is conserved with an accuracy of a few parts in 1000.

However, one should also note that our calculation evaluates the wave function as a whole and that is why it also contains a portion that remains bound on the timescales shown in our illustrations. We think that the tiny variations in the total probability transported by the pulse actually reflect the finite accuracy achieved in our calculation and that the temporal variations of the bound part of the wave function are small in comparison. So keeping in mind the finite accuracy of the calculation, it is reasonable to say that these pulses represent mostly particles that are escaping toward infinity.

In order to visualize the particle trajectory, Fig. 7 shows the probability density plotted versus time and observation location. One can see that the particle's probability density concentrates along the parabola reflecting its classical acceleration. However, the slope at the intersection with the red horizontal line which marks x_{exit} indicates that the particle appears here delayed and with a nonzero velocity. Interestingly, the figure also brings to light that a well-defined wave packet forms before it reaches the classical exit point from the tunnel. In effect, there seems to be a distribution of the tunnel exits [39] and corresponding velocities.

This is similar to the Wigner tunneling picture [40], but in our case a range of energies contributes to the wave function giving rise to a fuzzy particle trajectory, with parameters potentially different from those calculated for a fixed-energy propagator [40] suitable for an adiabatic regime. Also note that ours is a nonadiabatic regime when mapping to a single classical trajectory may not be fully adequate [19].

Our results also illustrate that the wave packet exhibits a quite-well-defined duration, which can be perhaps surprising given that there is no inherent timescale imposed by the external field as there would be in the excitation by an optical pulse. However, one can appreciate that there is a natural timescale imposed by the energy spectrum of the states that contribute to the tunneling current. The broader the initial energy spectrum, the shorter the resulting particle pulse.

The duration of the emitted pulse is relevant for the applications of metal nanotips as superfast sources of electron bunches [36,41]. While ours is at best an idealized model for a fast electron source, it is reasonable to look at this result as an estimate for the "fastest achievable electron packet." Moreover, our illustration clearly shows that the resulting particle pulse consists of a spectrum of energies and accordingly suffers from dispersion which will spread out the pulse upon further propagation.

IV. DISCUSSION

This section is devoted to a brief discussion of a few technical issues relevant for the calculations underlying our results.

First of all, it should be emphasized that the above example represents a generic behavior that we have obtained for a number of various model settings. We have found that whenever the field strength is weak we see very pronounced deviations from the scenario of instantaneous tunneling.

Yet another aspect the reader might be wondering about is that the expected exponential decay of the metastable state born out of the initial stationary state is not evident in our results. The explanation has to do with the fact that we look at relatively weak field strengths; the evanescent tail of the initial bound state is exceedingly small at $x = x_{\text{exit}}$ unless its energy Q is close to the very top of the potential well. The outgoing probability current induced to this state by the external field also occurs on a much slower timescale and it therefore appears negligible on the background of the fast wave packet generated by the suddenly imposed field. For the given conditions, the decay rate of the metastable states energetically close to the initial wave function is of the order of 10^{-9}. The tunneling pulses seen in our examples exhibit velocities on the order of unity and result in a roughly 10^{-5} ionization rate, so their contribution dominates by about four orders of magnitude. However, it is possible to create situations in stronger fields where these slow and fast components of the tunneled wave function are comparable.

Finally, we touch upon the the nonadiabatic aspect of the tunneling dynamics seen in our calculations. Clearly, it is the instantaneous switching on of the field that is responsible for

the broad energy spectrum of the resulting wave function at time $t \to 0^+$. One could ask if a more adiabatic turning on of the field can result in a more sharply defined tunneling time. Intuition suggests that when the field is turned on slowly the higher-energy components of the resulting state will be reduced and consequently the wave packet will broaden more in time due to its smaller bandwidth. Moreover, the slow ramping of $F(t)$ introduces significant arbitrariness into the meaning of $t = 0$ because only a sudden switching on gives a clearly defined initial time for the evolution. So, while in terms of nonadiabaticity ours is a most extreme scenario that can only be approximated in an experiment, it shows that the way the system is excited introduces yet another aspect that complicates the notion of the classical barrier-traversal time.

V. CONCLUSION

We have presented an exactly solvable model for an electron tunneling from a metal nanotip exposed to an external field. Taking advantage of the non-Hermitian reformulation of the time-dependent problem, we were able to calculate the wave function for the field strengths that present a difficult challenge for more standard methods, including numerical solutions of the time-dependent Schrödinger equation. The time-dependent wave function revealed that the energy spectrum of the system imposes an inherent lower limit on the duration of the electron pulse emitted by the tip even when the field turns on suddenly. We have also seen that the energy spectrum of the emitted particle is wide and the tunneling wave packets therefore experience strong temporal dispersion.

However, our main motivation for this study was the currently debated question of the tunneling time, which some claim to be instantaneous, while others present evidence that it must be finite, and still others maintain that the quantum nature of the tunneling problem precludes a meaningful description in classical terms. As for the notion of the tunneling time, our results show that for our particular examples in one dimension and for a weak external field the tunneling dynamics exhibits a pronounced delay between the sudden switching on of the field and the time when the particle can be detected at the point of the classical exit from the potential barrier. Moreover, the so-called simple man's scenario of quantum tunneling also does not apply because the particle has a significant velocity when it appears at the classical exit point. So in this exactly solvable system one can safely say that the tunneling time is not instantaneous. However, our results do not support the idea of a well-defined tunneling time either. There are at least two reasons for this. First, it is obvious that at the point of classical exit, the temporal distribution of the probability density pulse is actually broader than the apparent tunnel time as defined by the time of arrival of the peak. In other words, the tunneling time is a stochastic quantity that perhaps could be better described by a probability distribution. Second, we have seen that a well-defined moving wave packet forms actually *before* the particle reaches the classically allowed region. In hindsight this is not very surprising given the energy uncertainty caused by the fast switching on of the field. Because of the energy spread, some components of the wave function experience the potential barrier as a classically accessible region. This makes the very notion of the tunnel exit rather ill-defined. By extension the utility of the tunneling time itself is limited at best. However, the time-dependent wave function exhibits a well-defined although fuzzy trajectory, and in this sense the behavior in our illustrations resembles the Wigner scenario [40]. The question of how the results of this paper compare *quantitatively* to Wigner's time is interesting, but is beyond the scope of the present work.

To conclude, we do not think that observations based on a simple one-dimensional model can be an arbiter in any way between the different schools of thought and experiments concerning the problem of the tunneling time. We hope, however, that the lessons learned from an exactly solvable system will help to shed additional light on the debate and that they will aid in building much needed intuition about the appropriate mix of quantum and classical in our understanding of the dynamics that play a role in a plethora of physical contexts.

ACKNOWLEDGMENTS

This work was based upon work supported by the Air Force Office of Scientific Research under Award No. FA9550-18-1-0183.

[1] E. Merzbacher, Phys. Today **55**(8), 44 (2002).
[2] L. Mandelstam and M. Leontowitsch, Z. Phys. **47**, 131 (1928).
[3] G. Gamow, Z. Phys. **51**, 204 (1928).
[4] L. A. MacColl, Phys. Rev. **40**, 621 (1932).
[5] F. T. Smith, Phys. Rev. **118**, 349 (1960).
[6] M. Büttiker and R. Landauer, Phys. Rev. Lett. **49**, 1739 (1982).
[7] R. Landauer and T. Martin, Rev. Mod. Phys. **66**, 217 (1994).
[8] M. Büttiker, Phys. Rev. B **27**, 6178 (1983).
[9] P. Eckle, M. Smolarski, P. Schlup, J. Biegert, A. Staudte, M. Schöffler, H. Muller, R. Dorner, and U. Keller, Nat. Phys. **4**, 565 (2008).
[10] T. Zimmermann, S. Mishra, B. R. Doran, D. F. Gordon, and A. S. Landsman, Phys. Rev. Lett. **116**, 233603 (2016).
[11] A. N. Pfeiffer, C. Cirelli, M. Smolarski, and U. Keller, Chem. Phys. **414**, 84 (2013).
[12] U. Sainadh, H. Xu, X. Wang, A. Atia-Tul-Noor, W. C. Wallace, N. Douguet, A. Bray, I. Ivanov, K. Bartschat, A. Kheifets, R. T. Sang, and I. V. Litvinyuk, Nature (London) **568**, 75 (2019).
[13] H. Ni, U. Saalmann, and J.-M. Rost, Phys. Rev. Lett. **117**, 023002 (2016).
[14] H. Ni, U. Saalmann, and J.-M. Rost, Phys. Rev. A **97**, 013426 (2018).
[15] P. Eckle, A. N. Pfeiffer, C. Cirelli, A. Staudte, R. Dörner, H. Muller, M. Büttiker, and U. Keller, Science **322**, 1525 (2008).
[16] N. Camus, E. Yakaboylu, L. Fechner, M. Klaiber, M. Laux, Y. Mi, K. Z. Hatsagortsyan, T. Pfeifer, C. H. Keitel, and R. Moshammer, Phys. Rev. Lett. **119**, 023201 (2017).

[17] A. S. Landsman, M. Weger, J. Maurer, R. Boge, A. Ludwig, S. Heuser, C. Cirelli, L. Gallmann, and U. Keller, Optica **1**, 343 (2014).
[18] E. E. Serebryannikov and A. M. Zheltikov, Optica **3**, 1201 (2016).
[19] M. Klaiber, K. Z. Hatsagortsyan, and C. H. Keitel, Phys. Rev. Lett. **120**, 013201 (2018).
[20] M. Yuan, Opt. Express **27**, 6502 (2019).
[21] N. Yamada, Phys. Rev. Lett. **83**, 3350 (1999).
[22] D. Sokolovski and E. Akhmatskaya, Commun. Phys. **1**, 47 (2018).
[23] L. Torlina, F. Morales, J. Kaushal, I. Ivanov, A. Kheifets, A. Zielinski, A. Scrinzi, H. G. Muller, S. Sukiasyan, M. Ivanov, and O. Smirnova, Nat. Phys. **11**, 503 (2015).
[24] J. Tan, Y. Zhou, M. He, Y. Chen, Q. Ke, J. Liang, X. Zhu, M. Li, and P. Lu, Phys. Rev. Lett. **121**, 253203 (2018).
[25] N. Eicke and M. Lein, Phys. Rev. A **97**, 031402(R) (2018).
[26] I. A. Ivanov, C. H. Nam, and K. T. Kim, Sci. Rep. **7**, 39919 (2017).
[27] A. N. Pfeiffer, C. Cirelli, M. Smolarski, D. Dimitrovski, M. Abu-Samha, L. B. Madsen, and U. Keller, Nat. Phys. **8**, 76 (2012).
[28] E. P. Wigner, Phys. Rev. **98**, 145 (1955).
[29] E. Pollak and W. H. Miller, Phys. Rev. Lett. **53**, 115 (1984).
[30] D. Sokolovski, in *Time in Quantum Mechanics*, edited by J. G. Muga, R. Sala Mayato, and I. L. Egusquiza (Springer, Berlin, 2002), pp. 183–217.
[31] S. Kocsis, B. Braverman, S. Ravets, M. J. Stevens, R. P. Mirin, L. K. Shalm, and A. M. Steinberg, Science **332**, 1170 (2011).
[32] H. M. Wiseman, New J. Phys. **9**, 165 (2007).
[33] M. Klaiber, D. B. Canario, K. Z. Hatsagortsyan, and C. H. Keitel, arXiv:2003.13130.
[34] Y. Ban, E. Y. Sherman, J. G. Muga, and M. Büttiker, Phys. Rev. A **82**, 062121 (2010).
[35] G. Herink, D. Solli, M. Gulde, and C. Ropers, Nature (London) **483**, 190 (2012).
[36] M. Förster, T. Paschen, M. Krüger, C. Lemell, G. Wachter, F. Libisch, T. Madlener, J. Burgdörfer, and P. Hommelhoff, Phys. Rev. Lett. **117**, 217601 (2016).
[37] G. Garcia-Calderon, A. Mattar, and J. Villavicencio, Phys. Scr. **2012**, 014076 (2012).
[38] R. Xu, T. Li, and X. Wang, Phys. Rev. A **98**, 053435 (2018).
[39] H. Ni, N. Eicke, C. Ruiz, J. Cai, F. Oppermann, N. I. Shvetsov-Shilovski, and L.-W. Pi, Phys. Rev. A **98**, 013411 (2018).
[40] E. Yakaboylu, M. Klaiber, and K. Z. Hatsagortsyan, Phys. Rev. A **90**, 012116 (2014).
[41] W. P. Putnam, R. Hobbs, P. D. Keathley, K. K. Berggren, and F. X. Kärtner, Nat. Phys. **13**, 335 (2016).